



Numerical Analysis of Interfacial Failure Mechanism in Bonded Steel–Concrete Composite Connections

Pankaj Kumar¹ · Arnav Anuj Kasar² · Sandeep Chaudhary³

Received: 8 October 2022 / Accepted: 3 July 2023 / Published online: 12 July 2023
© Korean Society of Steel Construction 2023

Abstract

The formation of steel–concrete composites using individual steel and concrete elements is commonly ensured by two different connection techniques at connected interface level: mechanical connectors and structural adhesives. Among these two connection techniques, the use of structural adhesive for bonding steel and concrete elements is rapidly increasing; primarily owing to uniform transfer of stresses over the entire bonded area. The behaviour of bonded connection with change in adhesive bond layer thickness at the level of composite interface are analysed using finite element analysis under static loading to examine the ultimate strength and shear stresses. The failure governing parameters of bonded connections, such as engendered stresses in terms of von-mises and hydrostatic stresses at bearing ends of the composite interface along with changes in failure patterns (from adhesive to cohesive) are discussed. Also, the maximum engendered stresses along the failure plane for different bond layer thicknesses are examined. In case of one mm bond layer thickness the variation in shear stresses is very high along (39.28 MPa to 23.15 MPa) and perpendicular (34.62 MPa to 16.97 MPa) to the loading direction. While, the specimen with three mm thickness exhibits maximum load bearing capacity, it also has relatively smaller variation in shear stresses along (34.91 MPa to 21.72 MPa) and perpendicular (32.72 MPa to 17.20 MPa), which shows uniformity of stresses with increase in thickness. However, a further increase in the thickness of the bond layer results in reduction in the shear capacity of the specimen.

Keywords Steel–concrete composite · Structural adhesive · Bond layer thickness · Shear stress

1 Introduction

The development of the construction and infrastructure industry unwrap new frontiers for materials and structural engineers. The steel and concrete are the most common material in current construction industry. Detailed literature in numerous studies is available on concrete, steel, and reinforced concrete as a material as well as structural member to understand the behaviour under various loading conditions

(Foraboschi, 2019a, 2019b, 2020). Further, in modern age demand of new construction material is upsurging to maximum utilization of positive attributes of each material. Development of steel–concrete composite as a construction material plays a significant role to accomplish the modern construction demand. Steel–concrete composite due to its inherent advantages over non-composite as well as reinforced cement concrete (Kumar et al., 2017a) is being preferred as a construction material. The principal advantages are a higher strength to unit weight ratio, and more flexible construction (Bouazaoui et al., 2007; Ekenel et al., 2006). Other benefits include the higher ultimate strength of member, higher section modulus, more stiffness, and speedier construction (Ekenel et al., 2006; Ellobody, 2014; Souici et al., 2013). The ease in repair, strengthening, and retrofitting along with better aesthetics makes the structure durable as well as economical and acceptable (Kumar et al., 2017a, 2017b; Yu-Hang et al., 2014). The superior performance of bonded composite members to that of mechanically connected composite members has led to the widespread

✉ Pankaj Kumar
pankaj.nitjaipur@gmail.com

¹ Department of Civil Engineering, National Institute of Technology Nagaland, Chumukedima, Dimapur 797103, India

² Department of Civil Engineering, Sagar Institute of Science Technology and Research, Bhopal, Madhya Pradesh 462036, India

³ Discipline of Civil Engineering, Indian Institute of Technology, Indore, Simrol, Indore 453552, India

popularity of the former. Conventionally, the composite action in the steel–concrete composite members is achieved through mechanical connectors (Kumar & Chaudhary, 2019), which cause stress concentration at the connected interface owing to limited availability of connection area and exhibit poor fatigue life (Bouazaoui et al., 2007; Kumar et al., 2017a; Souici et al., 2013). Such connections are also unable to provide high degree of interaction or full interaction at the level of composite interface, even at the maximum level of application of mechanical shear connector. Also, the application of higher number of mechanical connectors may result improper alignment of reinforcement bars in terms of centre to centre spacing and may induces improper placement of concrete. To resolve the deficiencies of mechanical connectors, a suitable solution for connection is structural adhesives. The efficacy of structural adhesives as a connecting material has been thoroughly researched to resolve the shortcomings of mechanical connectors.

The literature suggests that the application of structural adhesives as connector at composite interface meets the requirement of current age. Which involves multi-material design approach to construct structural member as efficient and economical solution (Mette et al., 2016). The effectiveness of structural adhesives as a bonding agent between steel and concrete interfaces has been, and is still, a subject matter of research. Owing to the pressure sensitive nature of structural adhesives, the connection behaviour, ultimate strength, and failure mechanism of connections varies significantly with changes in thickness of bond layer. The change in ultimate strength is also evident with the variation in bond area (length and width), specimen geometry and type of stresses that the connection is experiencing. The influence of bond layer thickness on connection behaviour is more intervening and rapid. Specially, when the bonded area length is relatively shorter. The influence of thickness is critical along the loading direction. The higher thickness of connected elements (adherends) results in failure of brittle nature (Silva & das Neves et al., 2009). Geometric aspect of adherend thickness has been studied by Leffler et al. (2007) and Silva et al. (2009). They suggest that the deformation traction relation does not depend on the thickness of elements need to connect, owing to its low infiltration depth of stress (Bhardwaj et al., 2021a; Leffler et al., 2007; Silva & das Neves et al., 2009). As earlier stated, the change in bonded area and specimen geometry changes the strength of connection, even the connection experiencing same kind of loading/stresses. Mechanical properties of adherends also change the failure mechanism and ultimate strength, load proportion factor and shear stress factors (Bhardwaj et al., 2021a, 2021b).

The adhesive layer thickness influence on bonded connection is studied by several researchers. There is no unambiguous judgement on the influence of change in adhesive layer thickness. Some researchers (Derewonko et al., 2008; Silva

& das Neves et al., 2009) reported that an increment in adhesive layer thickness at bonded area/at interface level causes an increase in bond strength, while some others reported that an increase in adhesive layer thickness at bonded area decreases the bond strength (Bouazaoui et al., 2007; Çolak, 2001; Çolak et al., 2009; Kahraman et al., 2008; Kumar et al., 2018). The threshold level attainment under pull-out test for steel–concrete composite (reinforcement bar inserted in concrete cylinder) was attained by Colak (2001). He suggested that the bond strength increases up to adhesive layer thickness of two mm and start decreasing after this point. Detailed experimental study on bond layer thickness of adhesive was conducted by Kumar et al. (2018). Authors conducted a comprehensive study on steel–concrete composite push out test specimens under compressive loading. The study shows an increase in up to a certain bond layer thickness (three millimetre) and after three millimetres, the change in bond layer thickness shows decrement in connection strength.

The variation of stresses in adhesive layer was reported by Silva et al. (2009) and Derewonko et al. (2008). The conducted studies reported that the structural adhesive with thin bond layer show high stress intensity or depict high shear stress concentration. Owing to this high stress concentration the bonded adhesive connection fails at relatively lower applied load level. The failure behaviour analysis shows at composite interface early attainment of ultimate/failure strain prior to the initiation of stress dispersion in surrounded area. Other similar studies conducted by Schnerch et al. (2007) and Buyukozturk and Hearing (1998) on composite connection behaviour. The magnitude of stresses generated in the adhesives at the edge of bonded joint in shear and peeling shows significant change with the change in applied thickness of adhesive (Schnerch et al., 2007). The authors examine the failure mode of composite connection in retrofitted reinforced concrete flexural member. The results show that the change in adhesive layer thickness affects the failure mode. The common modes of failure in retrofitted reinforced concrete beams are flexural compression, shear, layer expulsion in concrete, and delimitation of fibre reinforced polymer (Buyukozturk & Hearing, 1998). As an extension of previous study, concrete-adhesive-fibre reinforced polymer composite bonded system with varying concrete element strength investigated by Lopez-Gonzalez et al. (2012). The study shows that the correction estimation of bonded connection is only possible when adhesive and adherends, both have almost same strength and, the failure governed by the composite interface. If adherends is the weakest component in component in composite, the failure always happens in weakest component and bond layer thickness of adhesive does not affect the strength of connection significantly. The interfacial failure varies with change in adhesive layer thickness, owing change in stress

redistribution capacity with the change in thickness of adhesive layer (López-González et al., 2012).

The possible reason behind slack in connection integrity in terms of effectiveness is variation in thickness. Thus, the adhesive connection with lesser bond layer thickness increases the connection efficiency. The increase in connection efficiency shows positive influence on bond strength (Cognard et al., 2005; Frigione et al., 2006). And, also shows increase in connection efficiency in terms of connection capacity (ultimate strength) and in terms of stiffness/rigidity (degree of interaction) (Jurkiewicz et al., 2011). The variation in bond strength in shear loading (Mode-II) was examined by Stigh et al. (2014). The outcome of conducted study shows linear increment in the compliance (flexibility) with change (increase) in the thickness of adhesive bond layer.

A study conducted by Martiny et al. (2012) find that the fracture energy of connection associated with adhesive bonded metallic connection. The study is conducted on bonded connection experiencing peel loading (Mode I). The results show adverse effect on bond fracture energy with the increment in adhesive layer thickness, which is used to forge a connection between metal surfaces. A similar parametric study on variation in fracture energy with the change in adhesive layer thickness conducted on Aluminium substrates by Cooper et al. (2021). The reported results suggested that energy associated with fracture in bonded connection changes with the change in bond layer thickness. Initially, the change in fracture energy is proportional to the bond layer thickness and it remains constant beyond a certain thickness of bond. A complete study on peel and shear mode was conducted by Carlberger and Stigh (2010). They observed a relation between the fracture energy associated in Mode I and II (peel and shear mode) and adhesive layer thickness. The relationship is proportional up to a certain level of bond layer thickness beyond which the fracture energy in both (shear and peel) modes decreases with increase in bond layer thickness.

The influence of adhesive layer thickness in metallic connection is studied by Zhao and Zhang (2007). They present a comprehensive review on carbon fibre reinforced polymer strengthened steel members. The study suggests that failure modes are strongly influenced by bond layer thickness. Cohesive connection failure was found in thin layered adhesives. Whereas an increase in thickness changes the failure mode from cohesive to complete adhesive or a combination of adhesive and cohesive mode. Among all, behaviour of steel–concrete composite connection interface in detail has not been studied in light of shear performance. Kumar et al. (2018) and Kumar (2013) carried out preliminary experimental investigations to study the feasibility of adhesive-bonded composite connection and composite interface. The vertical push-out test on steel–concrete composite bonded specimens was

performed in accordance with EC4 (EC4 & Eurocode4, 2004) and the study conducted to find the bond capacity and ultimate shear strength for the adhesive layer. Another aim to conduct experimental study was to find the influence of bond layer thickness on connection failure mechanism. The experimental study conducted by Kumar et al. (2018) shows a good correlation between adhesive bond layer thickness, connection shear capacity, and failure mechanism. They found that the connection shear capacity increases upto a certain limit of adhesive layer thickness, which was three mm. After three mm, the connection capacity is dropping from its maximum value. The failure mode also varies with the change in adhesive layer thickness. Initially, the connection fails in adhesive mode up to two mm of thickness. After two mm, the failure mode changes from adhesive to mixed (adhesive and cohesive) and from mixed to cohesive. The variation of connection shear strength and connection stiffness is shown in Fig. 1.

2 Need of the Study

The literature presents a broad outlook about connection strength, stress variation at bonded interface, and failure mechanism of metal–metal, metal–composite, metal–fibre, and fibre–fibre composite interface with the variation in adhesive layer thicknesses. The connection strength of bonded steel–concrete composite specimen with variation in bond layer thickness has been investigated in detail. But, the stress variation and interfacial behaviour of connection has not been yet presented. Therefore, the variation in bond strength as well as stresses at composite interface is considered in current study. A parametric numerical study is conducted on push-out test specimens using finite element software ABAQUS (ABAQUS, 2013). The stress variation of bonded area (along the length and width) or composite interface are plotted. The amount of maximum and minimum stresses is also reported.

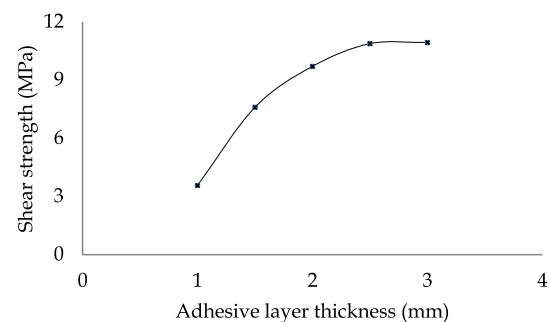


Fig. 1 Change in shear strength with bond layer thickness for steel–concrete composite connection

3 Material Modelling

The mechanical properties of materials along with their mathematical models for finite element analysis are listed in this section in details. The accuracy of finite element analysis depends on adequate modelling of the material behaviour. The steel–concrete composite specimen consists of three independent elements, namely, concrete slab, steel column section, and structural adhesive.

3.1 Concrete

The effective finite element simulation of concrete requires adequate estimation of linear and non-linear behaviour of material in terms of mathematical model. Several standard material models exist to capture the behaviour of concrete, such as, Drucker-Prager model, Mohr- Coulomb Plasticity model, Smeared Cracking model, Concrete Damaged Plasticity model. The present study requires adequate estimation of compressive and tensile behaviour of concrete. Concrete, as a material, exhibits entirely different properties in compression and tension. The propagation of cracks along with the post-cracking behaviour of concrete is a critical parameter that governs the selection of appropriate analytical model.

The elastic behaviour of concrete has been modelled in ABAQUS (ABAQUS, 2013) as a linear elastic material model with isotropic hysteretic properties. The value of density, elastic modulus, and Poisson’s ratio have been assigned. In compression, the value for elastic range (stress is directly proportional to strain) is $0.4f_u$. Beyond this limit, the plastic behaviour of concrete in the present study is simulated using the Concrete Damaged Plasticity (CDP) model. The model uses the concepts of isotropic damaged elasticity in combination with isotropic plasticity (tensile and compressive) to incorporate the inelastic behaviour of concrete. The CDP model assumes that the two main failure mechanisms in concrete are the compressive crushing and the tensile cracking. The compressive behaviour of concrete, in the inelastic region, has been incorporated in CDP model using behaviour suggested by Carreira and Chu (1985). The expression for uniaxial compression given in Eqs. 1 and 2, are

Table 2 Compressive strength and flexure strength of concrete after 7 and 28 days

IS designation	Compressive strength (MPa)		Flexural strength (MPa)	
	7 days	28 days	7 days	28 days
M 60	61.33	73.46	5.39	5.64

$$\frac{\sigma^c}{f_u^c} = \frac{\left(\epsilon^c / \epsilon_f^c\right) \gamma_c}{\gamma_c - 1 + \left(\left(\epsilon^c / \epsilon_f^c\right)^{\gamma_c}\right)} \tag{1}$$

$$\gamma_c = \frac{1}{1 - \left(f_u^c / E_{ic} \epsilon_f^c\right)} \tag{2}$$

where σ^c is compressive stress of concrete, ϵ^c is compressive strain in concrete, f_u^c is stress corresponding to strain ϵ_f^c

Under uniaxial tension, the stress–strain response of concrete remains linear in the elastic range followed by a brittle yield at failure stress, beyond which, microcracking in concrete initiates. This microcracking leads to strain localization at the section, that is mathematically represented by softening response in the stress–strain relationship. The tensile behaviour of concrete as suggested by Carreira and Chu (1985) has been employed to model the elasto-plastic material characteristics.

An experimental study was conducted to predict the concrete material behaviour and to validate the numerical model. Concrete mix proportioning is carried out in accordance with the ACI 211 (Committee Report 211.1, 2002) specifications. The concrete is prepared using PPC cement with 10 mm and 20 mm coarse aggregates, along with Zone II sand; fine aggregate as specified in the BIS 383 (Standard, BIS:383, 2016), regular tap water, and superplasticizer. Ratio of ingredients for concrete mix proportioning and quantity of ingredients per cubic meter are shown in Table 1.

3.1.1 Compressive and Flexure Strength

The compressive strength and flexure strength tests are performed on 150 mm size cubes, and 100 mm × 100 mm × 500 mm size beams cured for 7 days and 28 days. for all concrete. The average compressive strength

Table 1 Ratio of ingredients for concrete mix proportioning

	Cement	Sand	Aggregate		Water	Plasticizer
			10 mm	20 mm		
Ratio	1.00	1.14	1.81	1.20	0.32	1.51
(kg/m ³)	457.00	521.89	823.34	550.23	146.24	6.86

(f_{ck}) and flexure strength (f_{ct}) of concrete at 7 days and at 28 days, as observed, are reported in Table 2.

3.1.2 Modulus of Elasticity

The modulus of elasticity for the prepared grade of concrete is evaluated by conducting compression test on 150 mm × 300 mm standard specimens, as prescribed in ASTM C469/C469M (Standard, ASTM. C469/C469M, 2014). The deformation in concrete specimens is measured using one compressometer in longitudinal direction and one extensometer in lateral direction. The stress dependent loading rate of (0.241 ± 0.034 MPa/s) is maintained during the entire testing process. The applied load and the corresponding strain (longitudinal and lateral) are measured (1) at the longitudinal strain of 0.00005, and (2) at the load of 40% of the ultimate load. The modulus of elasticity is calculated using Eq. (3) suggested by ASTM C469/C469M (Standard, ASTM. C469/C469M, 2014), as given below,

$$E_c = \frac{(\sigma_{c2} - \sigma_{c1})}{(\epsilon_2 - 0.00005)} \tag{3}$$

where, σ_{c1} is the stress corresponding to longitudinal strain ϵ_1 of 0.00005, and σ_{c2} & ϵ_2 are stress and strain corresponding to a load level of 40% of the ultimate load. The elastic modulus obtained using Eq. (3) is reported in Table 3.

3.2 Structural Steel

A material model of structural steel is defined to effectively simulate the behaviour of steel elements in composite specimens. An elasto-plastic strain hardening model is employed to capture the structural steel behaviour.

3.2.1 Tensile Strength Test

The tensile strength tests are carried out on coupons cut from flange and web of steel sections. The tensile test specimens, with circular cross-section, are prepared in accordance with the BIS 1608 (Standard, BIS 1608, 1608). The schematic geometry and dimensional details of mild steel coupon are shown in Fig. 2. A strain dependent loading rate of 70 $\mu\text{m/s}$ is maintained for the entire testing process. The yielded coupon is shown in Fig. 3, a standard failure mechanism is observed with the formation of the neck near the middle portion of gauge length. For all

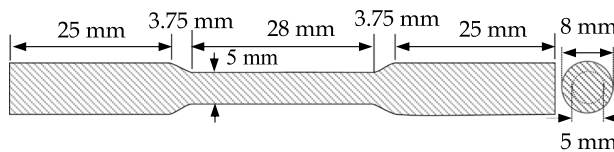


Fig. 2 Side view and cross-sectional view of circular tensile test coupon

the coupons, a cup-cone type failure is observed. Table 4 presents the mechanical properties (average) of tested coupons. The tested coupons have an average yield (0.2% offset) strength of 262.83 MPa and an ultimate strength of 423.67 MPa. Also, the tensile strain at initiation of elongation and ultimate failure are obtained as 0.0136 and 0.319, respectively. Figure 4 shows applied load elongation curve of tensile test coupon.

3.2.2 Elastic Behaviour

The elastic part of the material model is defined as linear with isotropic hysteretic properties. The value of density, elastic modulus and Poisson’s ratio are assigned, as obtained through the tests carried out on the individual material specimens. The elastic behaviour of steel is defined to be governed by Eq. (4).

$$\sigma_{ts} = \epsilon_{ts} E_s \tag{4}$$

where σ_{ts} is the stress in steel at any instance, ϵ_{ts} is the strain in steel at corresponding stress level, E_s is the Young’s modulus of steel.

3.2.3 Plastic Behaviour

The plastic part of the material behaviour is defined using a tri-linear model, representing the plastic region (having a strength plateau) and the strain hardening region (increasing strength with a gentle slope), upto the ultimate strain (0.189 for structural steel). The stress–strain curve for structural steel coupon is shown in Fig. 5. The values or coordinates of tri-linear points are determined from experimental values detailed in Table 4.

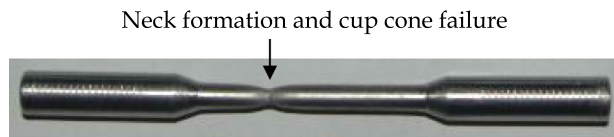


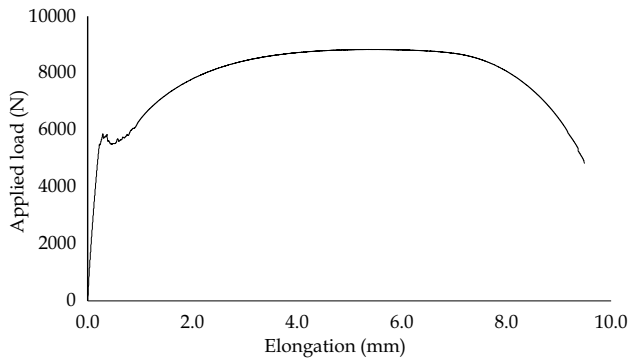
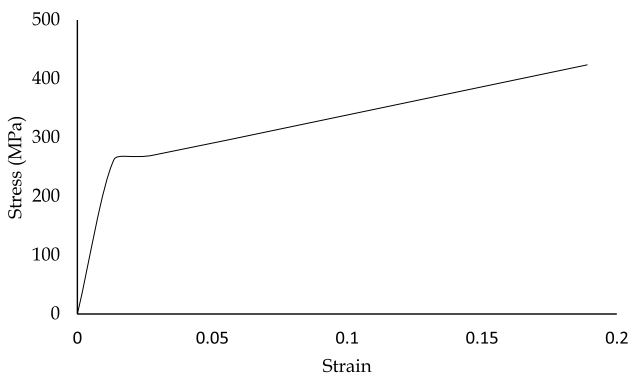
Fig. 3 Tensile test coupon after failure

Table 3 Elastic modulus of concrete along with concrete grades

Designation	C
IS designation	M 60
Elastic Modulus (MPa)	38,981

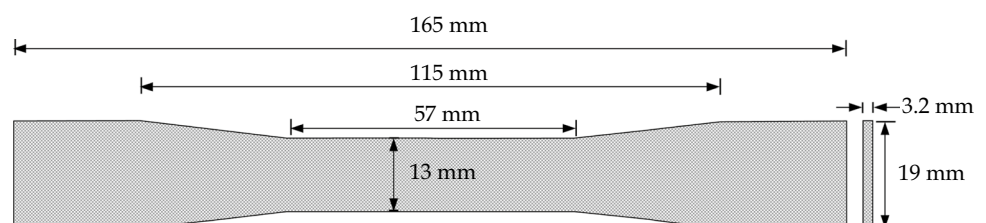
Table 4 Tensile properties of coupons obtained from steel sections

Elastic modulus (MPa)	Yield stress (MPa)	Yield strain	Ultimate stress (MPa)	Ultimate strain	Failure strain	Elongation (mm)
2,002,263.05	262.83	0.0136	423.67	0.189	0.319	8.93

**Fig. 4** Applied load-elongation curve for steel coupon under tensile loading**Fig. 5** Idealised tri-linear stress-strain curve for structural steel coupon

3.3 Structural Adhesive

The simulation of behaviour of epoxy adhesive in finite element analysis is carried out using linear Drucker-Prager model. The use of von-mises yield criteria along with hydrostatic stress sensitivity in the linear Drucker-Prager model effectively captures the mechanical behaviour of epoxy adhesive. Standard tests are carried out to determine the

Fig. 6 Geometric details and shape of bulk epoxy adhesive specimen for tensile test

tensile and compressive strength of selected structural adhesive. The details of the same are presented in this section.

3.3.1 Tensile Strength Test

Tensile strength tests on bulk epoxy specimens are carried out as per ASTM D 638 (Standard, ASTM. D 638, 2014) using prismatic coupons. The geometric details of rigid adhesive coupon for tensile test are shown in Fig. 6. Strain based tensile load is applied on the specimen at a constant rate of 17 $\mu\text{m/s}$. Figure 7a, b shows the photographs of the specimen during the test and after failure. Figure 8 shows the obtained stress-strain curve for bulk epoxy adhesive. The curve shows that the stress-strain relationship of bulk epoxy follows an almost linear path up to failure. The behaviour of epoxy adhesive under tensile loading is unyielding (inflexible). The results of tensile test of bulk epoxy specimens, as reported in Table 5.

3.3.2 Compressive Strength Test

Compressive strength tests on bulk epoxy specimens are performed as per ASTM D695 (Standard, ASTM. D 695, 2015) specifications. Five identical cylindrical specimens of diameter 12.7 mm and height 25.4 mm are subjected to compressive load in universal testing machine (UTM). A constant strain rate of 17 $\mu\text{m/s}$ is applied. Figure 9a shows a schematic view of bulk epoxy cylindrical specimen, along with the geometric details. Figure 9b, c show the epoxy specimen subjected to compressive loading and the brittle failure of the specimen respectively. It can be observed that the failure plane is inclined at an angle of 45° from load bearing (horizontal) face representing shearing failure. The results of the compressive tests are presented in Table 6 and the stress-strain behaviour of epoxy specimen is shown in Fig. 10.

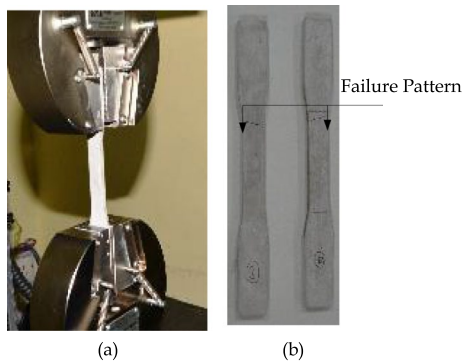


Fig. 7 Bulk epoxy specimen subjected under tensile loading in servo control universal testing machine and failed specimen, (a) epoxy specimen subjected under tensile loading in UTM and (b) epoxy specimen after tensile failure

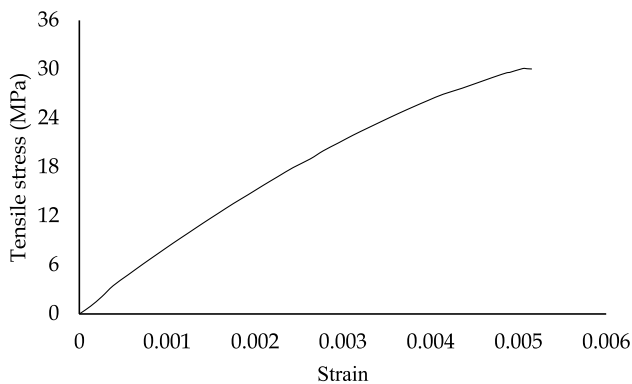


Fig. 8 Load-elongation curve for bulk epoxy adhesive specimen under tensile loading

Table 5 Tensile test results of bulk epoxy specimen

Yield stress (MPa)	Yield strain (mm/mm)	Ultimate stress (MPa)	Ultimate strain (mm/mm)	Failure strain (mm/mm)	Elastic modulus (MPa)
–	–	30.08	0.00496	0.00515	7551.88

4 Test Geometry and Methodology

4.1 Test Geometry

The behaviour of steel–concrete composite specimens under direct shear is evaluated using push-out test. For this purpose, small-scale composite specimens are prepared in the laboratory, and subjected to vertical push (compressive shear) such that the shear forces are introduced at the connecting interfaces, and consequently transferred from one element to another through the connection. With the

application of load, a relative slip is observed between the steel and concrete elements, because of deformation in connection material. The push-out test specimens can be performed by two different methods, namely, (1) horizontal push out test, in accordance with BIS 11384 (Standard, BIS 11384, 2022) and (2) vertical push out test in accordance with BS 5400 Part I (Standard, BS 5400 Part I, 2007), EC4 (Standard, Eurocode 4, 2004) and IRC 22 (Standard, IRC 22, 2015). In the present study, vertical push out tests are carried out to determine the connection behaviour.

4.1.1 Vertical Push-Out Test

The vertical push-out test specimens consist of a steel column of size UC 152@37 kg/m, of length 350 mm having bonded structural adhesive on both the flanges with reinforced concrete slab on each side (350 × 300 × 100) The standard arrangement of a push-out test specimen as per EC4 (2004) is shown in the Fig. 11.

The effect of bond layer thickness on the performance of connections is analysed through vertical Push-out Test specimen. A parametric numerical study, with specimens having five different bond layer thicknesses of 1 mm, 2 mm, 3 mm, 4 mm, and 5 mm is conducted. Five different values of thicknesses provide an insight on the failure modes of connection interfaces in the specimens. The finite element (FE) analysis software package ABAQUS (ABAQUS, 2013) is used. All elements (concrete slab, steel section and adhesive layer) are modelled as three-dimensional elements to increase computational accuracy. A uniform mesh is developed using three dimensional eight-noded brick elements with reduced integration (C3D8R). Owing to the symmetry of the push-out specimens in terms of loading, boundary conditions and geometry, a quarter model is analysed to simulate the experimental conditions. To model the quarter part of push out test specimen half concrete slab (350 Height × 150 Width × 100 Depth) is modelled with zero displacement on continuous edge. Quarter part of steel section with half web thickness is modelled with zero displacement on continuous surface. Half of the adhesive layer is modelled. The details of the modelled specimens along with boundary conditions are shown in Fig. 12. Different mesh sizes have been tried to achieve the convergence of FE analysis results.

5 Validation with Experimental Results

The verification of the numerical model has been carried out by comparing the results obtained from Finite Element (FE) analysis and experimental (push-out test) results published by Kumar et al. (2018). Figure 11 shows the geometry of an experimental push-out test specimen. Since the geometry of push-out test specimens is symmetric about both the X- axis

Fig. 9 Compressive testing; **a** side and cross-sectional view of circular compressive test specimen **b** specimen subjected under compressive loading and **c** specimen after failure

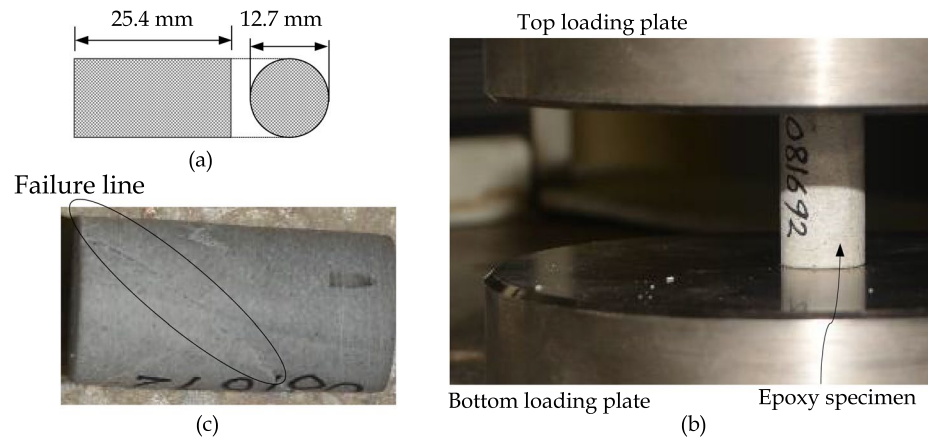


Table 6 Compressive test results of bulk epoxy specimen

Yield stress (MPa)	Yield strain (mm/mm)	Ultimate stress (MPa)	Ultimate strain (mm/mm)	Failure strain (mm/mm)	Elastic modulus (MPa)
73.94	0.0129	82.073	0.0228	0.0517	7537.78

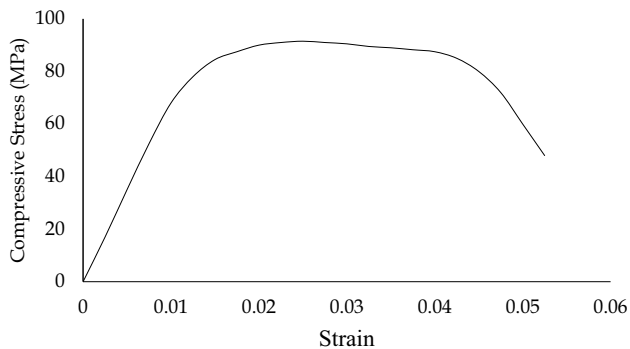


Fig. 10 Compressive stress–strain curve for bulk epoxy adhesive specimen under compressive loading

and Y-axis, thus, to reduce the computational effort quarter finite element model is prepared (as shown in Fig. 12). Since this is a validation study, only the steel–concrete composite push-out test specimen with three mm bond layer thickness is modelled. The ultimate capacity along with relative slip of bonded specimen has been compared with experimental results obtained by Kumar et al. (2018). Figure 13 shows a comparison of the load–slip curve obtained through finite element analysis and experimental investigation. It is evident from Fig. 13 that both finite element analysis and experimental study performed by Kumar et al. (2018) are in close agreement with each other. The maximum obtained values for applied load and relative slip along with variations in ultimate values are reported in Table 7. The maximum attained values for applied load (ultimate strength)

and relative slip in FE Analysis are about 123.46 kN and 27.90 μm ; as compared to the corresponding experimental values of 119.96 kN and 32.91 μm , respectively. The variations in ultimate strength and relative slip are about 2.83% and 17.95%, respectively. The high variation in relative slip in experimental study conducted by Kumar et al. (2018) and FE Analysis are attributed to the uncertainty in experimental results.

6 Results and Discussion

The results have been obtained for half of the adhesive layer width and for remaining half width same results are considered. Firstly, the ultimate strength of bonded steel–concrete composite push-out test specimen in terms of maximum shear stress with bond layer thickness were plotted for all five thicknesses. Further, the maximum shear stresses of the interfacial adhesive layer, between steel and concrete elements, in terms of the variation in shear stress along the length and width of the layer, are discussed in this section. The effects of variation in thickness of adhesive layer are underlined.

6.1 Bond Strength Variation in Connection

Maximum load applied over the bonded composite push-out test specimens, bonded area, and magnitude of shear stresses in terms of ultimate strength are outlined in Table 8. The graphical representation for the variation in bond shear strength with respect to the thickness of adhesive layer is presented in Fig. 14. The results suggest that with an increase in thickness of adhesive layer the shear capacity of bonded connection increases up to a thickness of three mm. The increment in shear strength is found to be 17.18%, from 10.24 to 12.00 MPa with increase in thickness from one mm to three mm, respectively. However, for the thicknesses of adhesive layer beyond three

Fig. 11 Steel–concrete composite vertical push-out specimen bonded with adhesive as per EC4 (2004); **a** top view and **b** side view

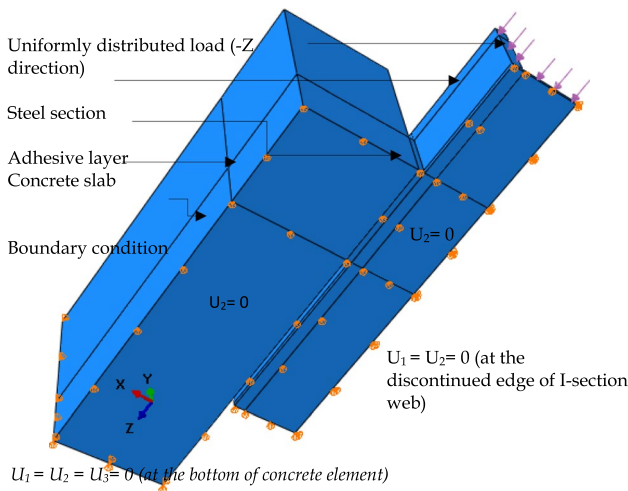
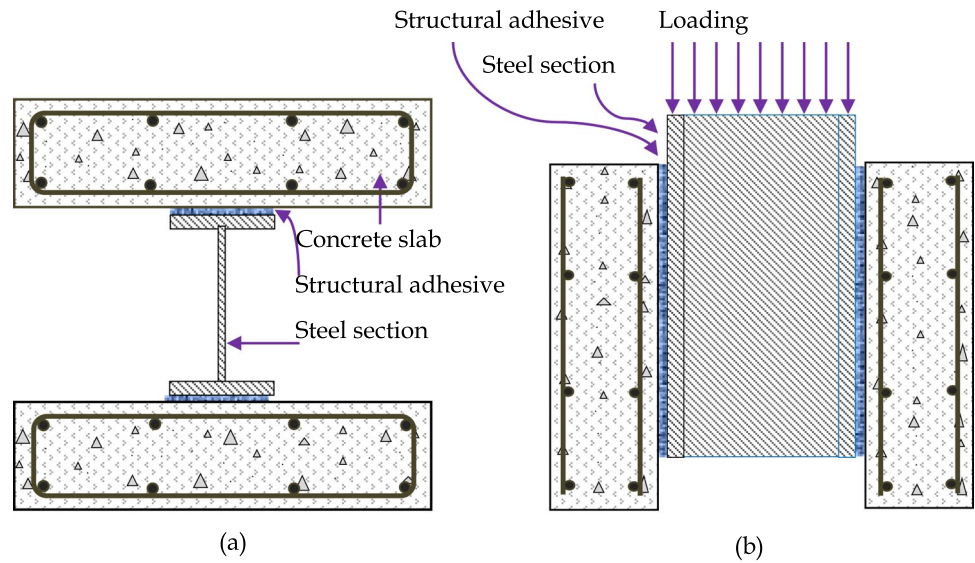


Fig. 12 Geometric details of FE quarter model of steel–concrete composite Push-out test specimen

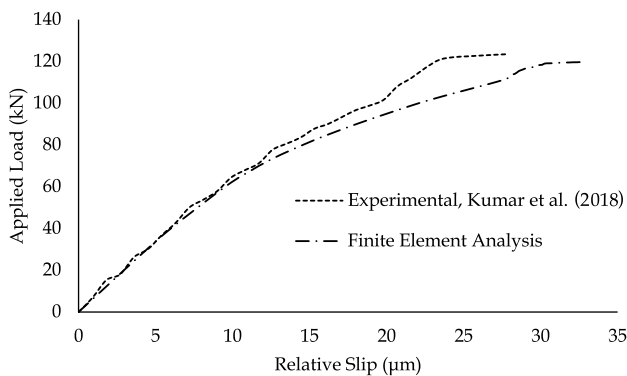


Fig. 13 Variation of relative slip with applied load curve for three mm thick adhesive layered steel–concrete composite specimen

Table 7 Comparison in bond strength—relative slip curve of steel–concrete composite push-out test specimen obtained from experimental study by Kumar et al. (2018) and FE analysis

	Experimental (Kumar et al., 2018)	Finite element analysis	Variation (%)
Applied load (kN)	123.46	119.96	2.83
Relative slip (μm)	27.90	32.91	17.95

Table 8 Bond strength of steel–concrete composite push-out test specimen with bond layer thickness

Adhesive layer thickness (mm)	Maximum load (N)	Bonded area (mm ²)	Ultimate strength (N/mm ²)
1	102,395.51	10,000	10.24
2	107,401.23	10,000	10.74
3	119,956.79	10,000	12.00
4	102,185.18	10,000	10.22
5	92,950.62	10,000	9.30

mm, the connection strength is observed to decrease. The decrease in shear strength is 22.50%, from 12.00 to 9.30 MPa with increase in thickness from three to five mm, respectively. This reduction can be attributed to the concentration of stresses along the edges of the bonded area. The higher concentration of stresses at the steel–matrix–concrete interface at edge leads to shear yielding of connections having thinner adhesive layers (1 mm and 2 mm), while for adhesive layers having thicknesses of 3 mm and beyond the failure is attributed to the pressure sensitive behaviour of the adhesive leading to development of high hydrostatic tension in adhesive layer.

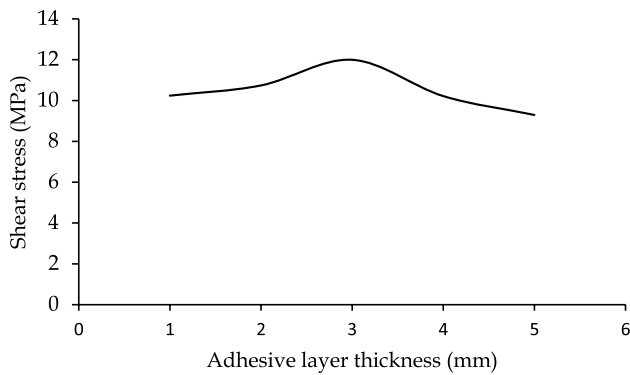


Fig. 14 Variation of bond strength with change in thickness of adhesive layer

6.2 Stress Variation in the Bonded Area

The variation of shear stresses along the length (z -axis) and width (y -axis) (Fig. 12), of the bonded area determines the behaviour of connections. The results of the finite element analyses are used to determine the distribution of shear stresses in the bonded area and to gain insight on the connection behaviour under compressive loading. For this purpose, the specimens with different thicknesses of adhesive layer (1 mm, 2 mm, 3 mm, 4 mm, and 5 mm) are analysed. The variations of shear stress (S_{xy} or S_{12}) across the width of the adhesive layers and shear stress (S_{xz} or S_{13}) across the length of the adhesive layer of each thickness are shown in Figs. 15, 16, 17, 18 and 19. The figures show the variation of shear stresses in the adhesive layer,

along the width of the bonded area (at the top, middle and bottom levels) and also along the length of bonded area (at the left, centre and the right edges) of the bonded width.

6.3 Bond Layer Thickness of one mm

The variation of shear stresses (S_{xy} or S_{12}) along the width and (S_{xz} or S_{13}) along the length of the bonded area are shown in Fig. 15. It is observed that along the width the top and bottom edges of the bonded area are subjected to maximum stresses. The maximum shear stress of -39.27 MPa is observed at the bottom of adhesive layer along the concrete bearing edge, while the maximum shear stress of -34.626 MPa occurs at the top surface of adhesive layer in the starting edge along the interface in the direction of loading. It is also observed that the magnitude of shear stresses in bonded area attains maximum magnitude at the bottom most edge. The concentration of stresses along the bonded edges is the most probable reason for the observed behaviour.

The failure occurs because the shear stresses surpasses the permissible value of shear stress along the bonded edges leading to shear yielding at the discontinuous edge. The comparison between stress variation along the top (black) and bottom (magenta) width of the model is evident in Fig. 15. The critical magnitude of shear stresses along the edges in general, and bottom edge in particular, leads to failure in the bonded interface.

Fig. 15 Variation in shear stresses along the width and length of the bonded area for one mm thickness

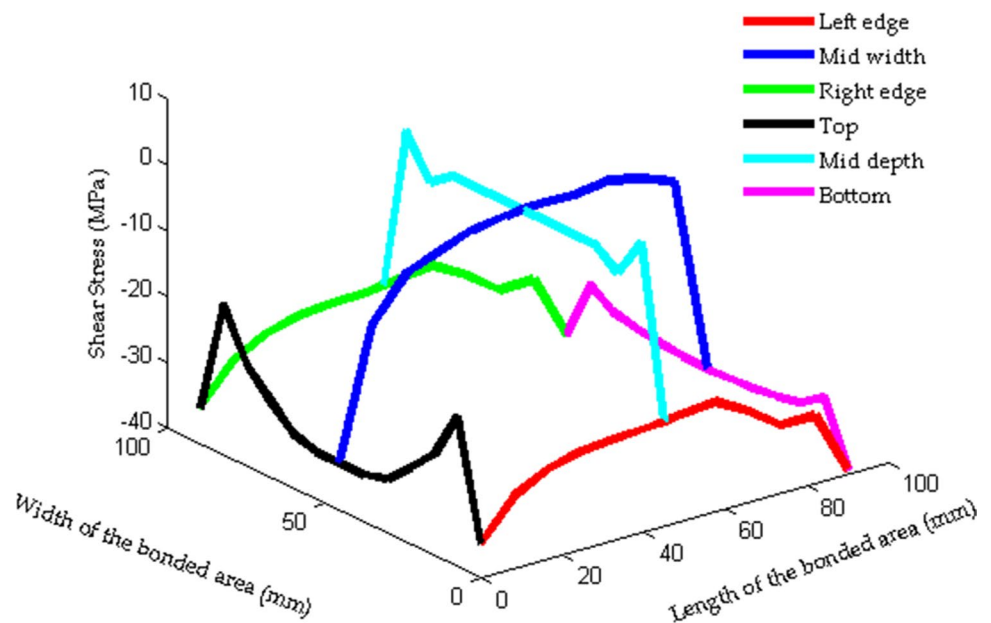


Fig. 16 Variation in shear stresses along the width and length of the bonded area for two mm thickness

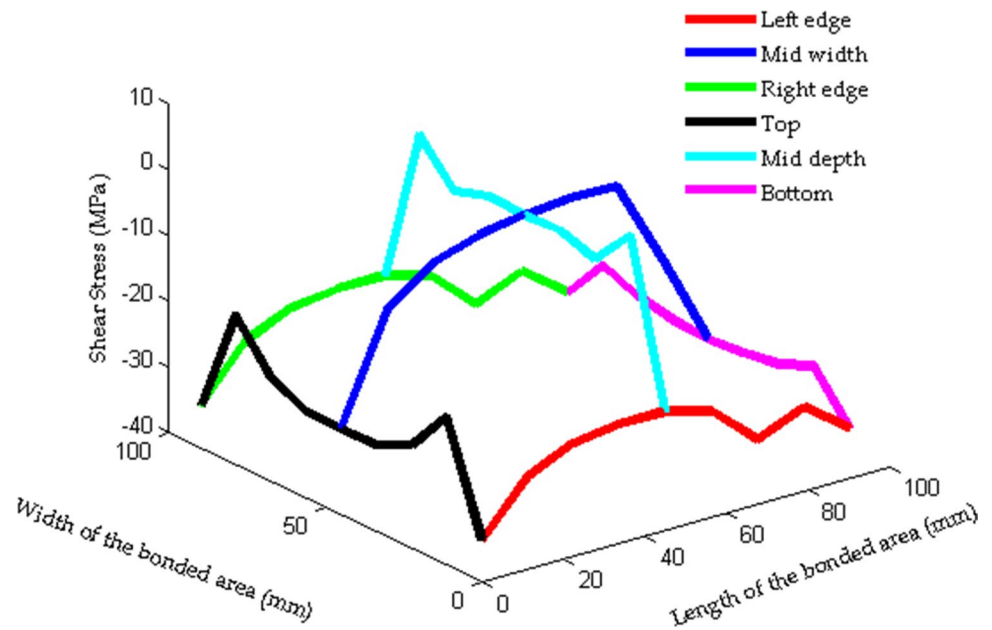
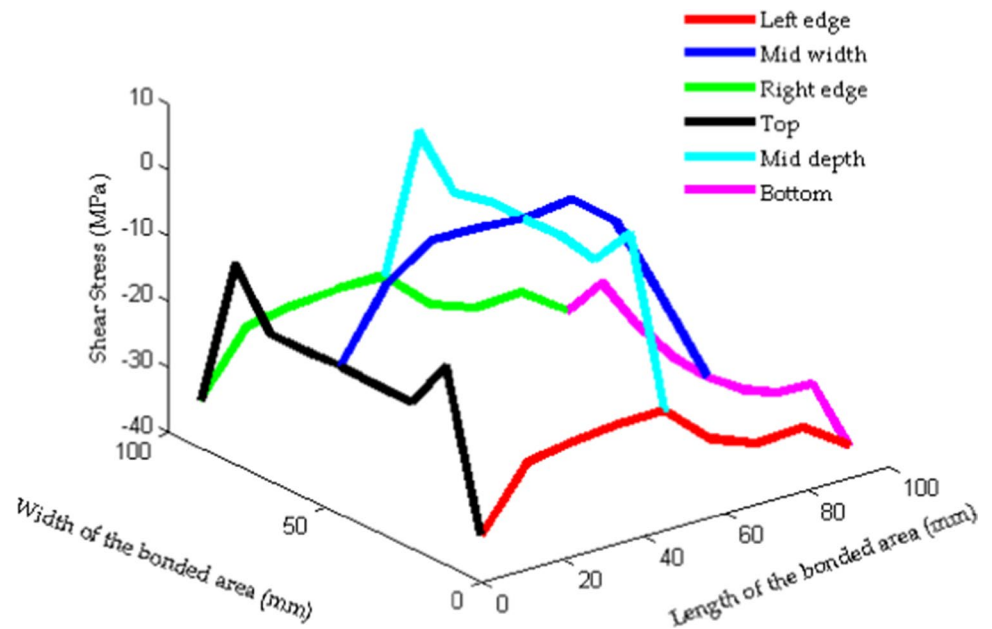


Fig. 17 Variation in shear stresses along the width and length of the bonded area for three mm thickness



6.4 Bond Layer Thickness of two mm

The variation of shear stresses (S_{xy} or S_{12}) along the width and (S_{xz} or S_{13}) along the length of the bonded area for the model having two mm thickness of adhesive layer is shown in Fig. 16. The observed *negative* maximum shear stresses at the top and bottom surfaces of the bonded area are 32.204 MPa (in the starting edge of the interface in the direction of loading) and 33.514 MPa (along the edge at the concrete bearing end), respectively. The observed magnitudes of shear stresses are lower as compared to one mm thick

bond layer. Nonetheless, the connection strength has been observed to increase (approximately 4.88%) from 10.24 MPa for one mm thick adhesive layer to 10.74 MPa for two mm thick adhesive layer. It shows that the concentration of shear stress reduces with increase of adhesive layer thickness. In case of both one mm and two mm thickness of adhesive layers, the failure is attributed to the increase in induced shear stresses beyond the permissible limit. However, the permissible stresses themselves vary due to hydrostatic condition, which leads to higher ultimate strength. The variation of shears stresses along the width of the adhesive layer at the

Fig. 18 Variation in shear stresses along the width and length of the bonded area for four mm thickness

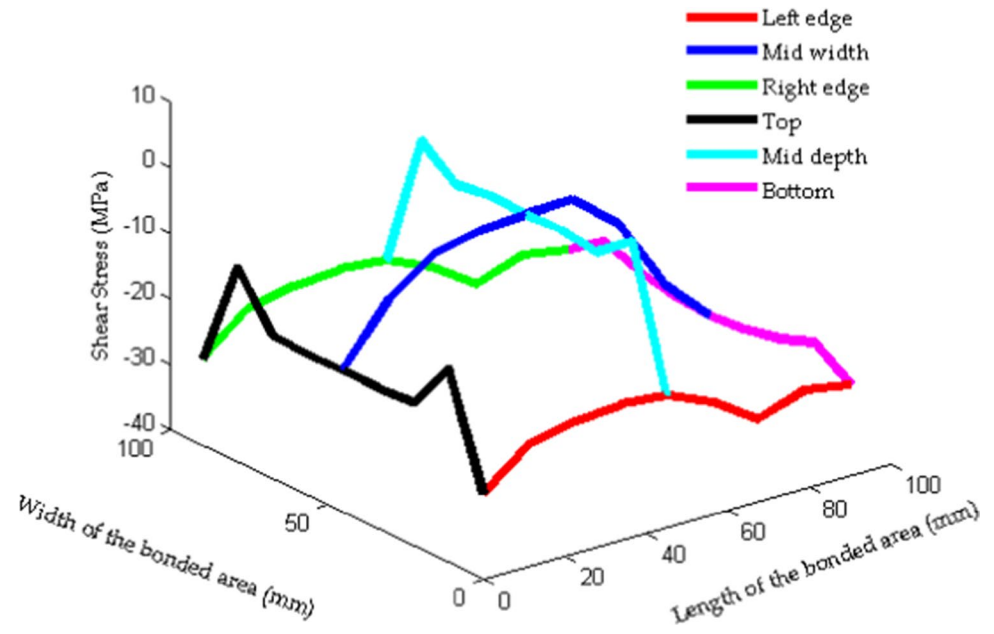
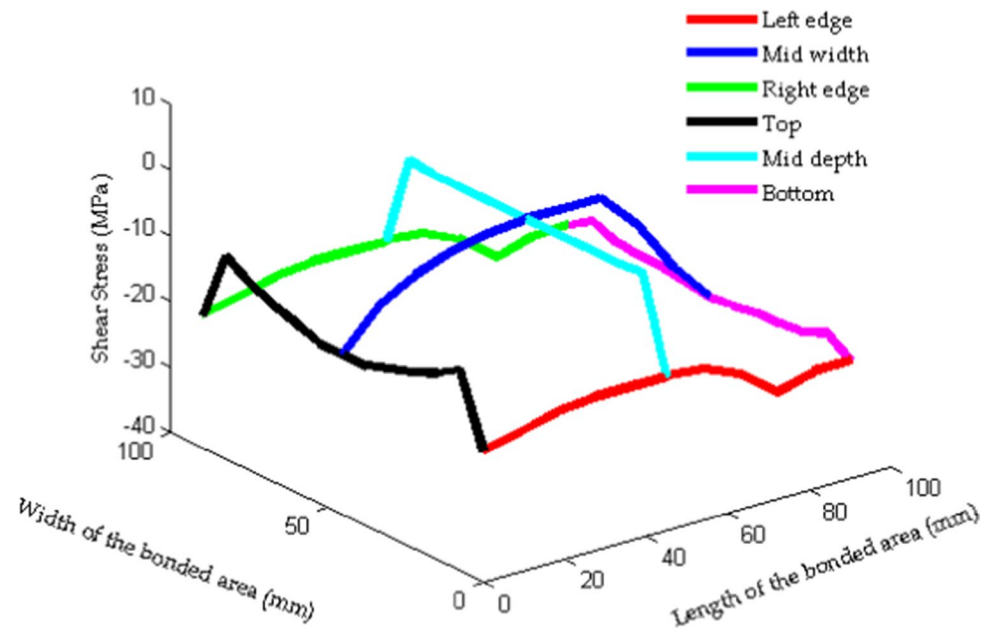


Fig. 19 Variation in shear stresses along the width and length of the bonded area for five mm thickness



top (black), middle (cyan) and bottom (magenta) levels are also shown in the Fig. 16. The comparative observation of the variation in shear stresses at the top and bottom surfaces of the adhesive layer along the width highlights the criticality of these edges in the determination of failure mode of the specimen model.

6.5 Bond Layer Thickness of three mm

The variation of shear stresses along the width and the length of the bonded area, for composite connection having three

mm thickness of adhesive layer, is shown in Fig. 17. The maximum shear stresses are observed at the edges of bonded area. The maximum shear stress at the top of the bonded area, along the starting edge of the interface in the direction of loading, is -32.717 MPa. Also, the maximum shear stress along the bottom edge of the of the bonded area is observed to be -34.91 MPa. The stress distribution profiles along the length and width of the adhesive layer exhibit a more uniform distribution of stresses over the entire bonded area. The results of the finite element analysis also suggest that the increase in thickness of adhesive layer from one mm to three mm leads

to an increase of 17.18% (from 10.24 to 12.00 MPa) in the connection strength. The reason of failure in this case is the increase in shear stress in the bonded area over the shear strength of the connection.

6.6 Bond Layer Thickness of four mm

Figure 18 shows the variation of shear stresses along the width and the length of the bonded area, for the composite connection having adhesive layer thickness of four mm. The figure suggests that the maximum shear stresses in the bonded area occur at the top – 26.839 MPa and the bottom – 25.965 MPa edges, along the width of the specimen model. The results suggest that for the four mm thickness of adhesive layer, the shear stresses are distributed uniformly along the width of the bonded area. Also, the maximum stresses observed in this case are significantly lesser than those observed for lower thicknesses of the adhesive layers. However, the bond strength of the composite connection having four mm thickness of adhesive layer is observed to be lower than that of three mm thick adhesive layer by approximately 14.82%. The ultimate behaviour in case of higher thicknesses of adhesive layers is governed only by the properties of the adhesive used, owing to increasingly uniform distribution of stresses. The pressure sensitivity of adhesive layer increases the magnitude of hydrostatic stresses and von-mises equivalent stresses.

6.7 Bond Layer Thickness of five mm

For the composite connections having bond layer thickness of five mm, the variation of shear stresses (S_{xy} or S_{12}) along the width and (S_{xz} or S_{13}) along the length of the bonded area are shown in Fig. 19. The maximum shear stresses along the width of the bonded interface are observed to be – 19.77 MPa at top edge (starting edge of bonded area in loading direction) and – 21.826 MPa at the bottom edge (concrete bearing end side). The stress variation along the bonded area exhibits the most uniform stress distribution, among all the considered cases (one mm to five mm). The failure mode in such cases occurs at the lower stress level and is governed by the interlayer stresses along the pressure sensitive adhesive layer. Similar nature of conclusions has been suggested in study conducted by Cognard et al. (2011) on bulk adhesive specimen. The study suggest that the adhesives are pressure sensitive in nature. The magnitude of Von-mises equivalent stresses and hydrostatic stresses changes with change in thickness of adhesive layer.

7 Conclusions

The behaviour of steel–concrete composite push-out test specimens under monotonic loading is investigated through finite element analysis. The failure mechanism of the steel–concrete

composite interfaces, having five different thickness of adhesive layers (one mm to five mm) are discussed in the light of the shear stress results obtained. The variations in bond strength as well as the shear stresses variation in the bonded area are also discussed to gain insight on the overall push-out behaviour. The primary conclusions drawn from the present study are:

- The bond strength of steel–concrete composite interface depends on the thickness of adhesive layer. The strength of adhesive bonded connections increases with an increase in thickness of adhesive layer upto certain level, which can be addressed as optimum thickness (three mm), beyond the optimum thickness (after three mm) the overall connection strength decreases with increase in bond layer thickness.
- The mode of failure of bonded connections varies from complete adhesive to mixed mode, and from mixed to complete cohesive mode with increase in thickness of adhesive layer.
- Edges of the bonded area are subjected to maximum shear stresses along their respective longitudinal and transverse direction of loading. However, in all cases, the maximum shear stresses are observed at the top and bottom bearing edges, across the direction of loading. The magnitude of shear stresses is maximum at the corners (all four) and decreases along the length and width of the bonded area towards the centre.
- The magnitude of maximum shear stress at corners decreases with increase in thickness of adhesive layer. This decrement in maximum magnitude is gradual up to optimum thickness, beyond which a steep decline in the magnitude of maximum shear stress is observed.
- With an increase in the thickness of the adhesive layer the difference in maximum and minimum values of shear stresses reduces. For instance, for the adhesive layer thickness of one mm the variation is 96.56%, while for the adhesive layer thickness of five mm, the variation is 87.40%.
- For lower thicknesses such as one mm, the concentration of stresses along the edges leads to high intensity of shear stresses.

References

- ABAQUS, ABAQUS 6.13 User's manual, Simulia, Dassault Systems, Providence, RI, (HKS, 2013).
- ACI Committee Report 211.1. (2002). *Standard practice for selecting proportions for normal, heavyweight, and mass concrete*. American Concrete Institute.
- Bhardwaj, A., Matsagar, V. A., Nagpal, A. K., & Chaudhary, S. (2021b). Bond behavior in flexural members: Numerical studies. *International Journal of Steel Structures*, 21(1), 225–243.
- Bhardwaj, A., Nagpal, A. K., Chaudhary, S., & Matsagar, V. (2021a). Effect of location of load on shear lag behavior of bonded

- steel–concrete flexural members. *Steel and Composite Structures*, 41(1), 123–136.
- Bouazaoui, L., Perrenot, G., Delmas, Y., & Li, A. (2007). Experimental study of bonded steel concrete composite structures. *Journal of Constructional Steel Research*, 63, 1268–1278.
- Buyukozturk, O., & Hearing, B. (1998). Failure behavior of precracked concrete beams retrofitted with FRP. *Journal of Composites for Construction*, 2, 138–144.
- Carlberger, T., & Stigh, U. (2010). Influence of layer thickness on cohesive properties of an epoxy-based adhesive—An experimental study. *The Journal of Adhesion*, 86, 816–835.
- Carreira, D. J., & Chu, K.-H. (1985). Stress–strain relationship for plain concrete in compression. *Journal Proceedings*, 82(6), 797–804.
- Cognard, J. Y., Bourgeois, M., Créac’Hcadec, R., & Sohier, L. (2011). Comparative study of the results of various experimental tests used for the analysis of the mechanical behaviour of an adhesive in a bonded joint. *Journal of Adhesion Science and Technology*, 25(20), 2857–2879.
- Cognard, J. Y., Davies, P., Gineste, B., & Sohier, L. (2005). Development of an improved adhesive test method for composite assembly design. *Composite Science and Technology*, 65, 359–368.
- Çolak, A. (2001). Parametric study of factors affecting the pull-out strength of steel rods bonded into precast concrete panels. *International Journal of Adhesion and Adhesives*, 21, 487–493.
- Çolak, A., Çoşgun, T., & Bakırcı, A. E. (2009). Effects of environmental factors on the adhesion and durability characteristics of epoxy-bonded concrete prisms. *Construction and Building Materials*, 23, 758–767.
- Cooper, V., Ivankovic, A., Karac, A., McAuliffe, D., & Murphy, N. (2021). Effects of bond gap thickness on the fracture of nano-toughened epoxy adhesive joints. *Polymer*, 53, 5540–5553.
- Derewonko, A., Godzimirski, J., Kosiuczenko, K., Niezgoda, T., & Kiczko, A. (2008). Strength assessment of adhesive-bonded joints. *Computational Materials Science*, 43(2008), 157–164.
- EC4, Eurocode 4. (2004). Design of composite steel and concrete structures. Part 1–1: General rules and rules for buildings, EN 1994-1-1, Brussels, Belgium.
- Ekenel, M., Rizzo, A., Myers, J. J., & Nanni, A. (2006). Flexural fatigue behavior of reinforced concrete beams strengthened with FRP fabric and precured laminate systems. *Journal of Composites for Construction*, 10, 433–442.
- Ellobody, E. (2014). *Finite element analysis and design of steel and steel–concrete composite bridges*. Butterworth-Heinemann.
- Foraboschi, P. (2019a). Lateral load-carrying capacity of steel columns with fixed-roller end supports. *Journal of Building Engineering*, 26, 100879.
- Foraboschi, P. (2019b). Bending load-carrying capacity of reinforced concrete beams subjected to premature failure. *Materials*, 12(19), 3085.
- Foraboschi, P. (2020). Predictive formulation for the ultimate combinations of axial force and bending moment attainable by steel members. *International Journal of Steel Structures*, 20(2), 705–724.
- Frigione, M., Aiello, M., & Naddo, C. (2006). Water effects on the bond strength of concrete/concrete adhesive joints. *Construction and Building Materials*, 20(2006), 957–970.
- Jurkiewicz, B., Meaud, C., & Michel, L. (2011). Non linear behaviour of steel–concrete epoxy bonded composite beams. *Journal of Constructional Steel Research*, 67, 389–397.
- Kahraman, R., Sunar, M., & Yilbas, B. (2008). Influence of adhesive thickness and filler content on the mechanical performance of aluminum single-lap joints bonded with aluminum powder filled epoxy adhesive. *Journal of Materials Processing Technology*, 205, 183–189.
- Kumar, P. (2013). Experimental investigations for shear bond strength of steel and concrete bonded by epoxy. [M. Tech. Dissertation]. Department of Civil Engineering, Malaviya National Institute of Technology Jaipur.
- Kumar, P., & Chaudhary, S. (2019). Effect of reinforcement detailing on performance of composite connections with headed studs. *Engineering Structures*, 179, 476–492.
- Kumar, P., Chaudhary, S., & Gupta, R. (2017b). Behaviour of adhesive bonded and mechanically connected steel–concrete composite under impact loading. *Procedia Engineering*, 173, 447–454.
- Kumar, P., Patnaik, A., & Chaudhary, S. (2017a). A review on application of structural adhesives in concrete and steel–concrete composite and factors influencing the performance of composite connections. *International Journal of Adhesion and Adhesives*, 77, 1–14.
- Kumar, P., Patnaik, A., & Chaudhary, S. (2018). Effect of bond layer thickness on behaviour of steel–concrete composite connections. *Engineering Structures*, 177, 268–282.
- Leffler, K., Alfredsson, K., & Stigh, U. (2007). Shear behaviour of adhesive layers. *International Journal of Solids and Structures*, 44, 530–545.
- López-González, J. C., Fernández-Gómez, J., & González-Valle, E. (2012). Effect of adhesive thickness and concrete strength on FRP-concrete bonds. *Journal of Composites for Construction*, 16, 705–811.
- Martiny, P., Lani, F., Kinloch, A., & Pardoën, T. (2012). A multi-scale parametric study of mode I fracture in metal-to-metal low-toughness adhesive joints. *International Journal of Fracture*, 173, 105–133.
- Mette, C., Stammen, E., & Dilger, K. (2016). Challenges in joining conductive adhesives in structural application—Effects of tolerances and temperature. *International Journal of Adhesion and Adhesives*, 67, 49–53.
- Schererch, D., Dawood, M., Rizkalla, S., & Sumner, E. (2007). Proposed design guidelines for strengthening of steel bridges with FRP materials. *Construction and Building Materials*, 21(2007), 1001–1010.
- Silva, L. F. M., das Neves, P. J. C., Adams, R. D., & Spelt, J. K. (2009). Analytical models of adhesively bonded joints—Part I: Literature survey. *International Journal of Adhesion and Adhesives*, 29, 319–330.
- Silva, L. F. M., das Neves, P. C., Adams, R. D., Wang, A., & Spelt, J. K. (2009). Analytical models of adhesively bonded joints—Part II: Comparative study. *International Journal of Adhesion and Adhesives*, 29, 331–341.
- Souici, A., Berthet, J., Li, A., & Rahal, N. (2013). Behaviour of both mechanically connected and bonded steel–concrete composite beams. *Engineering Structures*, 49, 11–23.
- Standard, BIS 11384. (2022). Composite construction in structural steel and concrete—Code of practice. Bureau of Indian Standards, New Delhi, India.
- Standard, BIS 1608. (2005). “Metallic materials—Tensile testing at ambient temperature. Bureau of Indian Standards, New Delhi, India.
- Standard, Eurocode 4. (2004). Design of composite steel and concrete structures—Part 1–1: General rules and rules for buildings, Brussels, Belgium
- Standard, ASTM. D 638. (2014). Standard test method for tensile properties of plastics. ASTM International, West Conshohocken, PA. <https://doi.org/10.1520/D0638-14>.
- Standard, ASTM. C469/C469M. (2014). Standard test method for static modulus of elasticity and poisson's ratio of concrete in compression. ASTM International, West Conshohocken, PA, 2010. https://doi.org/10.1520/C0469_C0469M-14
- Standard, ASTM. D 695. (2015). Standard test method for compressive properties of rigid plastics. ASTM International, West Conshohocken, PA. <https://doi.org/10.1520/D0695-15>

- Standard, IRC 22. (2015). Standard specifications and code of practice for road bridges Section VI: Composite construction (limit states design). Indian Roads Congress, New Delhi.
- Standard, BIS:383. (2016). Coarse and fine aggregate for concrete—Specification (Third Revision). Bureau of Indian Standards, New Delhi, India.
- Standard, BS 5400 Part I. (2007). Steel, concrete and composite bridges Part 1: General statement. British Standards Institution, London.
- Stigh, U., Biel, A., & Walander, T. (2014). Shear strength of adhesive layers—models and experiments. *Engineering Fracture Mechanics*, 129, 67–76.
- Yu-Hang, W., Jian-Guo, N., & Jian-Jun, L. (2014). Study on fatigue property of steel–concrete composite beams and studs. *Journal of Constructional Steel Research*, 94, 110.
- Zhao, X.-L., & Zhang, L. (2007). State-of-the-art review on FRP strengthened steel structures. *Engineering Structures*, 29, 1808–1823.

Publisher's Note Springer Nature remains neutral with regard to jurisdictional claims in published maps and institutional affiliations.

Springer Nature or its licensor (e.g. a society or other partner) holds exclusive rights to this article under a publishing agreement with the author(s) or other rightsholder(s); author self-archiving of the accepted manuscript version of this article is solely governed by the terms of such publishing agreement and applicable law.